

Electrochemical Synthesis of Zn–Al Layered Double Hydroxide (LDH) Films

Matthew S. Yarger, Ellen M. P. Steinmiller, and Kyoung-Shin Choi*

Department of Chemistry, Purdue University, West Lafayette, Indiana 47907, USA

Received January 30, 2008

A new electrodeposition condition to produce Zn–Al LDH films was developed using nitrate solutions containing Zn^{2+} and Al^{3+} ions. Deposition was achieved by reducing nitrate ions to generate hydroxide ions on the working electrode. This elevates the local pH on the working electrode, resulting in precipitation of Zn–Al LDH films. The effect of deposition potential, pH of the plating solution, and the Zn^{2+} to Al^{3+} ratio in the plating solution on the purity and crystallinity of the LDH films deposited was systematically studied using X-ray diffraction and energy dispersive spectroscopy (EDS). The optimum deposition potential to deposit pure and well-ordered Zn–Al LDH films was $E = -1.65\text{V}$ versus a Ag/AgCl in 4 M KCl reference electrode at room temperature using a solution containing 12.5 mM $\text{Zn}(\text{NO}_3)_2 \cdot 6\text{H}_2\text{O}$ and 7.5 mM $\text{Al}(\text{NO}_3)_3 \cdot 9\text{H}_2\text{O}$ with pH adjusted to 3.8. The resulting film contained 39 atomic % Al^{3+} ions replacing Zn^{2+} ions, leading to a composition of $\text{Zn}_{0.61}\text{Al}_{0.39}(\text{OH})_2(\text{NO}_3)_{0.39} \cdot x\text{H}_2\text{O}$. Increasing or decreasing the aluminum concentration in the plating solution resulted in the formation of aluminum- or zinc-containing impurities, respectively, instead of varying aluminum content incorporated into the LDH phase. Choosing an optimum deposition potential was important to obtain LDH as a pure phase in the film. When the potential more negative than the optimum potential is used, zinc metal or zinc hydroxide was deposited as a side product, whereas making the potential less negative than the optimum potential resulted in the formation of zinc oxide as the major phase. The pH condition of the plating solution was also critical, as increasing pH destabilizes the formation of the LDH phase while decreasing pH promoted deposition of other impurities.

Introduction

Layered double hydroxides (LDHs) are a group of inorganic materials that contain positively charged layers and charge balancing interlayer regions.¹ The composition of the main layer can be written as $[\text{M}(\text{II})_{1-x}\text{M}'(\text{III})_x(\text{OH})_2]$, with the positive charge on the main layer resulting from the replacement of divalent ions with trivalent ions. Both divalent and trivalent ions are located at the center of octahedra composed of OH^- ions; $\text{M}(\text{OH})_6$ and $\text{M}'(\text{OH})_6$ octahedral units share edges forming 2D layers. The interlayer incorporates anions and water molecules to maintain charge neutrality.

Because of its ability to accommodate various chemical species in the interlayer region, LDHs can serve as host materials to form a variety of intercalated and nanocomposite

compounds.² This ability can be used for a wide range of applications including catalysis, sensors, and drug/gene delivery.^{3–5} In particular, LDHs have been extensively used to prepare sensors to detect chemical and biological species (e.g., glucose, cholesterol, hydrogen peroxide, urea, and lactate).^{6–9} Using LDHs for sensing applications requires preparation of film-type LDH electrodes or adhesion of LDH powders to conducting substrates. The former can be achieved by spin coating or the Langmuir–Blodgett method, whereas the latter involves evaporation of colloidal LDH suspensions or use of carbon paste to glue powder-type LDHs to the electrode surface.^{6–14} These methods require a two-

* To whom correspondence should be addressed. Email: kchoi1@purdue.edu.

(1) de Roy, A.; Forano, C.; Besse, J. P. In *Layered Double Hydroxides: Present and Future*; Rives, V. Ed.; Nova Science Publishers: New York, 2001.

(2) Newman, S. P.; Jones, W. *New J. Chem.* **1998**, 22, 105.

(3) Del Hoyo, C. *Appl. Clay Sci.* **2007**, 36, 103.

(4) Evans, D. G.; Duan, X. *Chem. Commun.* **2006**, 485.

(5) Williams, G. R.; O'Hare, D. *J. Mater. Chem.* **2006**, 16, 3065.

(6) Forano, C.; Vial, S.; Mousty, C. *Curr. Nanosci.* **2006**, 2, 283.

(7) Darder, M.; Lopez-Blanco, M.; Aranda, P.; Leroux, F.; Ruiz-Hitzky, E. *Chem. Mater.* **2005**, 17, 1969.

(8) Mousty, C. *Appl. Clay Sci.* **2004**, 27, 159.

(9) Shan, D.; Cosnier, S.; Mousty, C. *Anal. Chem.* **2003**, 75, 3872.

step procedure involving synthesis of the LDH (e.g., coprecipitation method) followed by assembly of the electrodes.

In this study, we report a one-step electrochemical procedure to grow film-type Zn–Al LDH directly from a conducting substrate, which may allow for better physical adhesion between the LDH particles and the conducting substrate in addition to simplifying the assembly procedure. This method is based on electrochemical generation of OH[−] by reduction of nitrate ions (NO₃[−] + H₂O + 2e[−] → NO₂[−] + 2OH[−]).^{15,16} As the local pH on the working electrode increases, it provides for precipitation of the LDH only on the working electrode to form films. This method has been used previously by Kamath et al. to prepare Ni–Al, Ni–Mn, Mg–Al, and Mg–Cr LDHs and by Scavetta et al. to prepare Ni–Al LDH.^{17,18} However, zinc-based LDHs such as Zn–Al LDH, which have been used for sensing phenol, urea, and Ca²⁺ ions among others,^{7–9,19} have not been prepared by electrochemical deposition. This is mainly because electrochemical deposition of zinc-based LDHs interferes strongly with deposition of zinc metal and zinc oxide. In this study, we systematically investigated synthetic conditions that can enhance the purity and crystallinity of Zn–Al LDH during electrodeposition while suppressing deposition of other zinc-containing phases (e.g., ZnO, Zn(OH)₂, Zn). The study offers a foundation to establish conditions to prepare composite Zn–Al LDH electrodes containing various interlayer species by a one-step procedure.

Experimental Section

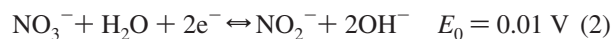
Electrodeposition. Zn–Al LDH films were electrodeposited using aqueous solutions containing 10–17.5 mM Zn(NO₃)₂·6H₂O (Aldrich, 98% purity) as the Zn²⁺ source and 2.5–10 mM Al(NO₃)₃·9H₂O (Alfa Aesar, 98% purity) as the Al³⁺ source. The solutions used in this work were prepared with DI water further purified with a Millipore Milli-Q purification system (resistivity ≥ 18 MΩ). The pH of the solutions was adjusted by adding NaOH and HNO₃ when necessary. A conventional three-electrode setup in an undivided cell was used (Princeton Applied Research VMP2 Multichannel Potentiostat/Galvanostat). Working electrodes were prepared by e-beam evaporation of 200 Å titanium and 600 Å of platinum, followed by 2000 Å gold on a cleaned glass substrate. For the counter electrode, a platinum foil electrode was used. The reference electrode was a Ag/AgCl electrode in 4 M KCl solution, against which all the potentials reported here were measured. Cathodic depositions were carried out at room temperature without stirring using −0.8 V ≤ E ≤ −1.8 V. After each deposition, the

resulting film was thoroughly rinsed with deionized water and dried with a gentle stream of nitrogen gas.

Characterization. X-ray diffraction (XRD) patterns were recorded on a Scintag X2 diffractometer (Cu Kα radiation). Scanning electron microscopy (SEM) images were obtained using a JEOL JSM-840 scanning electron microscope operated at 5 kV. The films were coated with gold and palladium using a thermal evaporator before imaging to minimize charging problems. Quantitative microprobe analysis was performed with a FEI-NOVA NanoSEM scanning electron microscope equipped with an Oxford Inca 250 EDS energy-dispersive spectroscopy detector to assess the amounts of zinc and aluminum present in as-deposited films. Fourier transform infrared (FTIR) spectra were collected using a PerkinElmer FTIR Spectrometer, model Paragon 500. The samples were prepared by scratching the film off the electrode and grinding it with oven-dried KBr (J.T. Baker) and pressed into a disk.

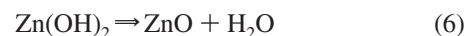
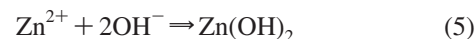
Results and Discussion

Deposition of Zn–Al LDH as a pure phase can be achieved when deposition of zinc metal and zinc oxide are effectively suppressed. Deposition of zinc metal involves reduction of Zn²⁺ ions while deposition of LDH requires generation of OH[−] ions by reduction of NO₃[−]. The standard reduction potentials of Zn²⁺ and NO₃[−] are shown in eqs 1 and 2.^{15,20}



The reduction of zinc metal requires a more negative potential than the reduction of NO₃[−] ions. Therefore, deposition of pure Zn–Al LDHs can be achieved by selecting a potential that is sufficient to reduce NO₃[−] ions but not enough to reduce Zn²⁺ ions for a given plating medium. The appropriate deposition potential must be determined based on the concentrations of Zn²⁺ and NO₃[−] ions as well as the solution pH because all of these factors can cause a significant shift in the reduction potentials of Zn²⁺ and NO₃[−] ions. It should be noted that in addition to nitrate reduction, hydrogen evolution reaction may also contribute to the decrease in pH by consuming H⁺ ions or generating OH[−] ions (2H⁺ + 2e[−] ⇒ H₂, 2H₂O + 2e[−] ⇒ H₂ + 2OH[−]).¹⁵

Avoiding deposition of ZnO is less straightforward than avoiding deposition of zinc metal because deposition of both ZnO and Zn(OH)₂ (the parent structure of Zn–Al LDH) is based on the reduction of NO₃[−] ions as shown below.



The only difference between the formation of ZnO and Zn(OH)₂ is the dehydration step (eq 6). This dehydration process is spontaneous and may not be explicitly controlled

- (10) Barhoumi, H.; Maaref, A.; Rammah, A.; Martelet, C.; Jaffrezic, N.; Mousty, C.; Vial, S.; Forano, C. *Mater. Sci. Eng., C* **2006**, *26*, 328.
 (11) He, J. X.; Kobayashi, K.; Takahashi, M.; Villemure, G.; Yamagishi, A. *Thin Solid Films* **2001**, *397*, 255.
 (12) Roto, R.; Yamagishi, A.; Villemure, G. *J. Electroanal. Chem.* **2004**, *572*, 101.
 (13) Shan, D.; Yao, W. J.; Xue, H. G. *Electroanalysis* **2006**, *18*, 1485.
 (14) Walcarius, A.; Lefevre, G.; Rapin, J. P.; Renaudin, G.; Francois, M. *Electroanalysis* **2001**, *13*, 313.
 (15) Therese, G. H. A.; Kamath, P. V. *Chem. Mater.* **2000**, *12*, 1195.
 (16) Yarger, M. S.; Steinmiller, E. M. P.; Choi, K. S. *Chem. Commun.* **2007**, 159.
 (17) Indira, L.; Kamath, P. V. *J. Mater. Chem.* **1994**, *4*, 1487.
 (18) Scavetta, E.; Mignani, A.; Prandstraller, D.; Tonelli, D. *Chem. Mater.* **2007**, *19*, 4523.
 (19) de Melo, J. V.; Cosnier, S.; Mousty, C.; Martelet, C.; Jaffrezic-Renault, N. *Anal. Chem.* **2002**, *74*, 4037.

by deposition potential. However, a recent study by Matsuoka and co-workers revealed that the formation of ZnO becomes more favorable as deposition temperature increases.²¹ Thus, for our intention to deposit Zn–Al LDHs, we investigated deposition conditions at room temperature.

In general, the ratio of the divalent to trivalent ions necessary to form a stable LDH phase ranges from 1:0.25 to 1:0.67.¹ As for Zn–Al LDH, the most commonly observed Zn^{2+} to Al^{3+} ratio is 1:0.33 to 1:0.5.^{13,22–24} Therefore, a solution containing 15 mM $\text{Zn}(\text{NO}_3)_2$ ions and 5 mM $\text{Al}(\text{NO}_3)_3$ ions ($\text{Zn}^{2+}/\text{Al}^{3+} = 3:1$) was prepared and used as the initial plating solution. The pH of the as-prepared plating solution was 3.8. Potentiostatic depositions were carried out at room temperature using various deposition potentials ($-0.8 \text{ V} \leq E \leq -1.8 \text{ V}$) to study the effect of the deposition potential on the phases of the deposits.

The film obtained at -0.8 V is white, and its XRD pattern shows two sharp peaks that are attributed to the wurtzite ZnO structure (part a of Figure 1). When the applied potential becomes more negative ($-1.2 \text{ V} \leq E \leq -1.4 \text{ V}$), the ZnO peak gradually decreases and a broad peak centered at approximately $2\theta = 10.5^\circ$ appears (parts b and c of Figure 1). This peak was assigned as the (003) reflection of Zn–Al LDH (space group $R\bar{3}m$; $00l$ reflections with $l \neq 3n$ are systematically absent) containing nitrate ions in the interlayer regions (nitrate ions are the only anions available in the plating solution that can be incorporated). The previous reported Zn–Al– NO_3 LDHs prepared by the solution coprecipitation method showed that a (003) reflection appeared at $9.8^\circ \leq 2\theta \leq 10.2^\circ$.^{22–24}

When the deposition potential reached -1.6 V , the color of the resulting film became gray. The XRD pattern of this film shows significantly enhanced (003) and (006) reflections of the LDH phase, confirming that this film contains Zn–Al LDH as the major phase (part d of Figure 1). This film, however, contains a new impurity phase, best assigned as hydrated zinc hydroxide ($\text{Zn}(\text{OH})_2 \cdot 0.5\text{H}_2\text{O}$) in addition to a trace amount of ZnO still present. Having only zinc-containing impurities at this condition suggests that the plating solution may lack Al^{3+} ions to form a pure Zn–Al LDH phase.

When the deposition potential was further increased to -1.8 V , both the peaks from Zn–Al LDH and zinc hydroxide gained intensity, whereas ZnO disappears, indicating that formation of hydroxide phases (both LDH and zinc hydroxide) becomes more favorable at more negative potentials (part e of Figure 1). At this potential, reduction of Zn^{2+} ions to zinc metal also occurred, and a new unidentifiable impurity peak appeared at $2\theta = 44.6^\circ$. These results suggest that the deposition potential of $E = -1.6 \text{ V}$

is optimal to inhibit the formation of impurity phases (e.g., zinc oxide, zinc hydroxide, and zinc) and to produce the purest Zn–Al LDH for a given plating solution. Therefore, we used the deposition potential of $E = -1.6 \text{ V}$ for further experiments to study the effect of pH and the composition of plating solutions on the purity and crystallinity of Zn–Al LDH films deposited.

The effect of the plating solution pH on the formation of the Zn–Al LDH phase was investigated by altering only the pH condition of the plating solution used in the previous section (pH 3.8). The pH was altered by adding either NaOH or HNO_3 . The XRD patterns of the films obtained from pH 4.3 and 3.0 are shown in Figure 2 in comparison with that from pH 3.8. At pH 4.3, $00l$ reflections of the LDH phase are no longer present, suggesting that increasing pH has an adverse effect on the stabilization of the LDH phase (parts a and b of Figure 2) at $E = -1.6 \text{ V}$. At pH = 3.0, the intensity of ZnO peaks is slightly reduced but other impurity phases appeared (e.g., zinc hydroxide, part c of Figure 2). The impurity peak appearing at $2\theta = 44.6^\circ$ is most likely generated by an aluminum-based or aluminum-rich phase, judging from the fact that this peak appears only when a significant amount of zinc-base impurities are formed (e.g., zinc hydroxide or zinc metal). The above results suggest that pH 3.8 is close to an optimum pH to form a pure and crystalline Zn–Al LDH phase and that increasing or decreasing pH from 3.8 may not be an effective way to suppress the formation of undesired impurities. This led to a supposition that increasing Al^{3+} concentration in a plating solution would be the most straightforward way to eliminate the zinc-related impurities (ZnO and $\text{Zn}(\text{OH})_2$).

On the basis of this assumption, two new plating solutions with a higher Al^{3+} content (solution II, $\text{Zn}^{2+}/\text{Al}^{3+} = 1:0.60$ and solution III, $\text{Zn}^{2+}/\text{Al}^{3+} = 1:0.77$) were prepared. The original solution ($\text{Zn}^{2+}/\text{Al}^{3+} = 1:0.33$) is referred to as solution I. The detailed compositions of solutions I–III are summarized in Table 1. The pH values of the as-prepared solutions were not consistent because the pH decreases as the amount of $\text{Al}(\text{NO}_3)_3$ increases. Therefore, the pH of these solutions was adjusted to 3.8 by adding a proper amount of NaOH before deposition. This assured that any changes observed in the resulting films were only due to varying the $\text{Zn}^{2+}/\text{Al}^{3+}$ ratio in the plating solutions and not due to any other factors. Depositions were carried out potentiostatically using a fixed potential of $E = -1.6 \text{ V}$ at 25°C .

The XRD patterns of the resulting films show two distinctive changes caused by increasing the amount of Al^{3+} in the plating solution (Figure 3). First, ZnO and $\text{Zn}(\text{OH})_2 \cdot 0.5\text{H}_2\text{O}$ impurities diminished, and both of the films obtained from solutions II and III exhibited XRD peaks originated from only the LDH phase. Second, the crystallinity of the LDH phase improves significantly, judging from the full width at half-maxima (fwhm) of the (003) and (006) reflection of LDH phase. This is due to the formation of a better-ordered LDH phase with more uniform basal spacings. When considering only the fwhm, solution III appeared to produce a Zn–Al film of a slightly better quality. However, to identify an optimum plating solution, elemental analysis

(20) Pourbaix, M. *Atlas of Electro-Chemical Equilibria in Aqueous Solutions*; Pergamon Press: New York, 1966.

(21) Otani, S.; Katayama, J.; Umamoto, H.; Matsuoka, M. *J. Electrochem. Soc.* **2006**, *153*, C551.

(22) Israeli, Y.; Taviot-Gueho, T.; Besse, J. P.; Morel, J. P.; Morel-Desrosiers, N. *J. Chem. Soc., Dalton Trans.* **2000**, 791.

(23) Radha, A. V.; Kamath, P. V.; Shivakumara, C. *J. Phys. Chem. B* **2007**, *111*, 3411.

(24) Zhang, L. Y.; Lin, Y. J.; Tuo, Z. J.; Evans, D. G.; Li, D. Q. *J. Solid State Chem.* **2007**, *180*, 1230.

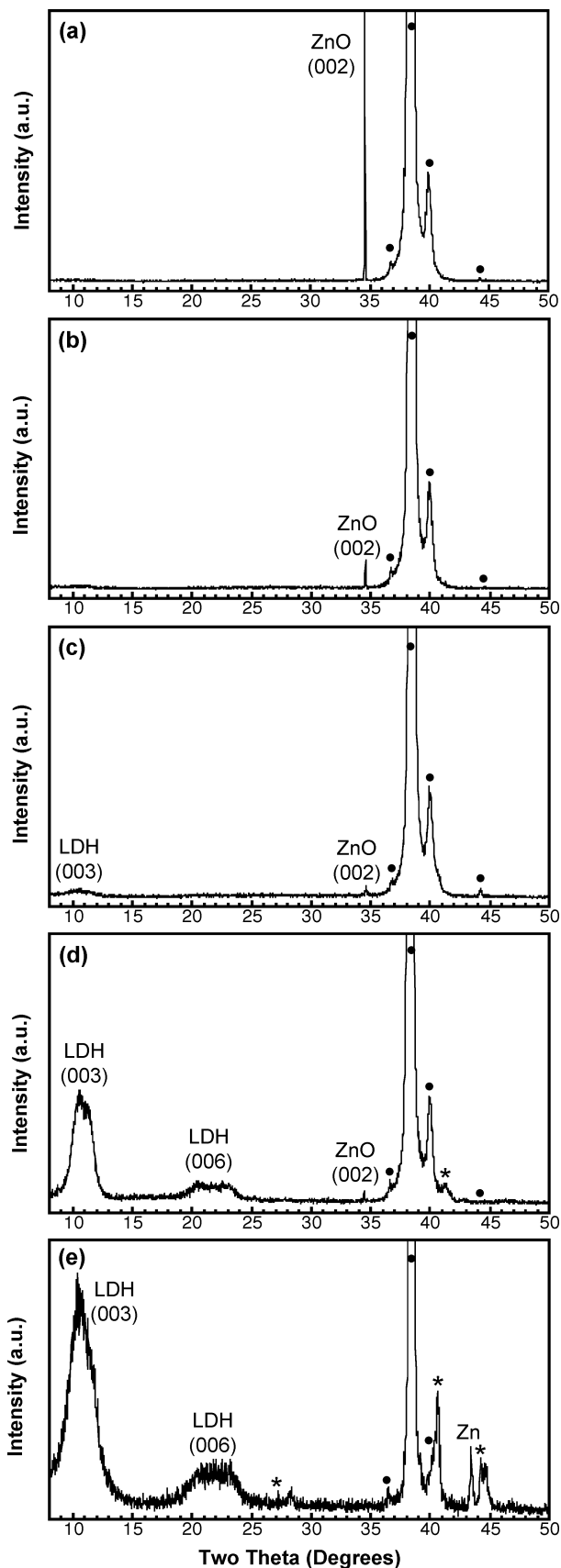


Figure 1. XRD of films deposited using a solution containing 1.5 mM $\text{Zn}(\text{NO}_3)_2$ and 0.5 mM $\text{Al}(\text{NO}_3)_3$ at (a) -0.8 V, (b) $E = -1.2$ V, (c) $E = -1.4$ V, (d) $E = -1.6$ V, and (e) $E = -1.8$ V. Peaks generated by the gold substrate are marked as (•), whereas peaks generated by $\text{Zn}(\text{OH})_2 \cdot 0.5\text{H}_2\text{O}$ are indicated by (*).

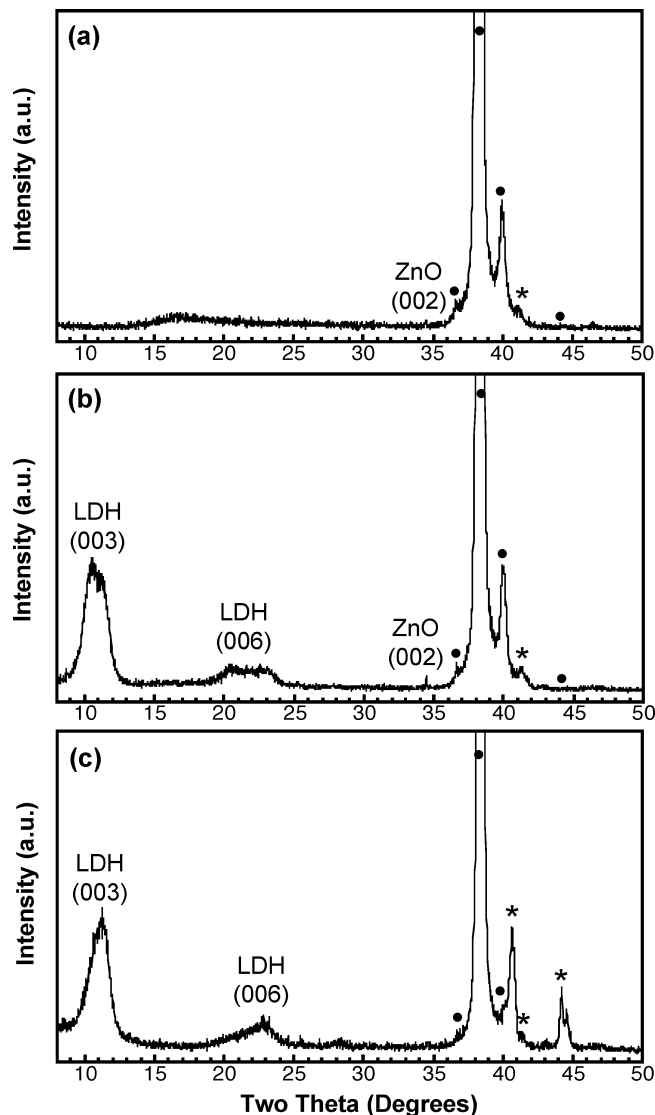


Figure 2. XRD of films deposited using a solution containing 1.5 mM $\text{Zn}(\text{NO}_3)_2$ and 0.5 mM $\text{Al}(\text{NO}_3)_3$ with pH adjusted to (a) 4.3, (b) 3.8, and (c) 3.0. The deposition was carried out at $E = -1.6$ V. The XRD patterns shown in part b of Figure 2 and in part d of Figure 1 are identical, but this pattern is shown again here for easy comparison for the effect of pH. Peaks generated by the gold substrate are marked as (•), whereas the peaks generated by $\text{Zn}(\text{OH})_2 \cdot 0.5\text{H}_2\text{O}$ are indicated by (*).

Table 1. Compositions of Plating Solutions and EDS Results of the Resulting Film Deposited from Each Solution

solution no.	Vol (mL) Used		molar ratio of Zn/Al in solution	atomic ratio of Zn/Al in film
	0.02 M $\text{Zn}(\text{NO}_3)_2$	0.02 M $\text{Al}(\text{NO}_3)_3$		
1	60	20	1:0.33	1:0.33
2	50	30	1:0.60	1:0.65
3	45	35	1:0.77	1:0.86

of the resulting films is necessary to confirm that these films do not contain any amorphous impurities that cannot be detected by XRD.

Results of the EDS analysis for films obtained from solutions I–III are summarized in Table 1. The film obtained from solution I shows a zinc to aluminum ratio of 1:0.33. Because the XRD pattern of this film shows the presence of zinc oxide and zinc hydroxide impurities in the addition to Zn–Al LDH (part a of Figure 3), some portion of zinc

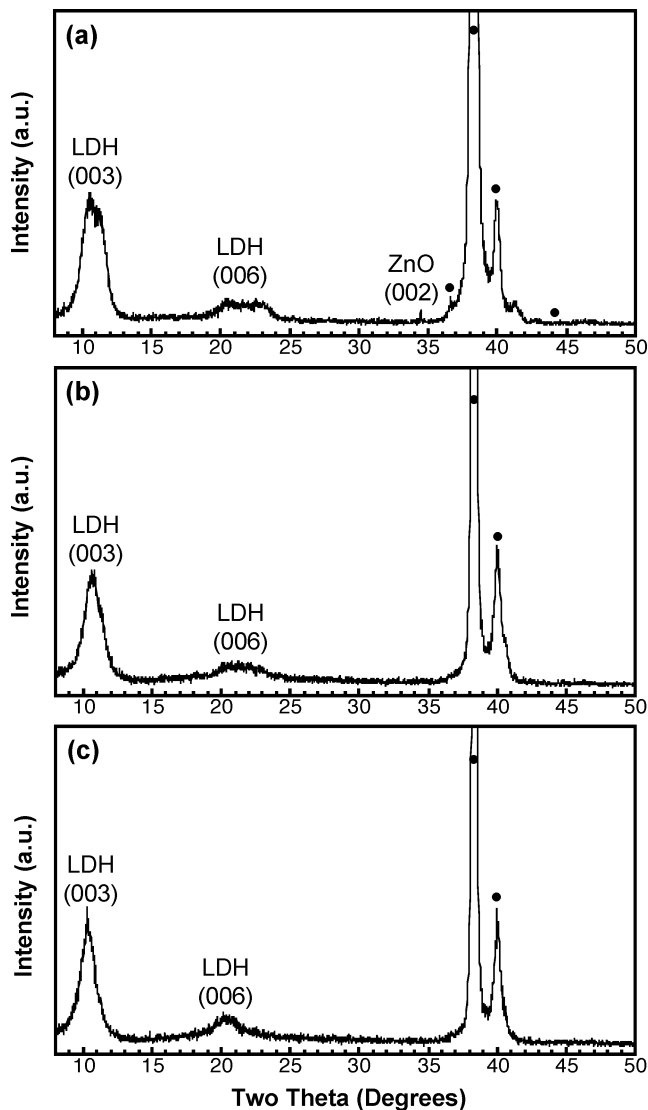


Figure 3. XRD of the films deposited from (a) solution I, (b) solution II, and (c) solution III at $E = -1.6$ V. The XRD patterns shown in part a of Figure 3 and part d of Figure 1 are identical, but this pattern is shown again here for easy comparison for the effect of solution compositions. Peaks generated by the gold substrate are marked as (*).

detected by EDS in this film is not from the LDH phase but from zinc-related impurities. Therefore, the actual zinc to aluminum ratio in the LDH film obtained from solution I should be smaller than 1:0.33 (i.e., more Al^{3+} per Zn^{2+}). The films prepared from solutions II and III both appear pure in the XRD patterns, but the EDS results show considerably different zinc to aluminum ratios for these films. Whereas the film from solution II contains a zinc to aluminum ratio of 1:0.65, the film from solution III contains a zinc to aluminum ratio of 1:0.86. If we assume that both of these films are pure Zn–Al LDH, their formulas are $\text{Zn}_{0.61}\text{Al}_{0.39}(\text{OH})_2(\text{NO}_3)_{0.39}$ and $\text{Zn}_{0.54}\text{Al}_{0.46}(\text{OH})_2(\text{NO}_3)_{0.46}$, respectively. The Zn^{2+} to Al^{3+} ratio of the film obtained from solution III is outside the typical divalent to trivalent ion ratio to form an LDH phase with reliable purity.¹ This suggests that this film may contain amorphous aluminum-containing impurities (i.e., aluminum hydroxide), although there is also a possibility that this film is composed of a

pure LDH phase with an unusually high aluminum content. Unfortunately, there is no straightforward method to know which case is true. Therefore, solution II, which generated Zn–Al LDH films with a Zn/Al ratio within the most reliable limit to form an LDH structure, was used to further improve the ordering of the LDH films (i.e., fwhm, crystallinity).¹

The very broad 00 l peaks of the Zn–Al LDH films are due to fluctuations in the basal spacing, which is most likely due to the inhomogeneous incorporation of aluminum into the layers and the resulting uneven content and distribution of the anions in the interlayer regions. To achieve a better ordering of LDH layers, the effect of deposition potential was investigated using solution II. Changing deposition potential allows for altering the rate of OH^- generation and therefore the local pH near the working electrode, which in turn can affect the precipitation rates of Zn^{2+} and Al^{3+} ions. Figure 4 shows XRD patterns of the LDH films deposited at varying deposition potentials (-1.5 , -1.6 , -1.65 , and -1.7 V). Decreasing the potential to -1.5 V did not cause any noticeable change in the purity and quality of the LDH phase. On the other hand, increasing it to -1.65 V significantly enhanced the intensity and the sharpness of the LDH peaks. Further potential increases to -1.7 V deteriorated the purity and ordering of the LDH films. Therefore, the best potential to deposit the purest and the most crystalline Zn–Al LDH film is -1.65 V.

The SEM images of the side and front views of the film deposited at -1.65 V using solution II are shown in Figure 5. The thickness of the LDH film can be controlled by deposition time. Typically, 3 min deposition results in a film of 4–5 μm thick under the given conditions. This clearly demonstrates the high deposition efficiency of producing LDH films by electrodeposition. The front view shows that the film has a smooth and featureless surface composed of domains of the lateral size of 200–300 nm.

FTIR spectra of the Zn–Al LDH film shows the presence of only nitrate ions and water in the interlayer region (Figure 6).^{25,26} The absorption peaks at 1384 and 832 cm^{-1} are due to the presence of nitrate ions, whereas the absorption peak at 1602 cm^{-1} is due to the presence of H_2O molecules in the interlayer region. A broad peak centered at 3453 cm^{-1} is generated by the O–H stretching of the LDH layer as well as interlayer water molecules.

The EDS analysis shows that the ratio between Zn^{2+} to Al^{3+} in the film is 1:0.65. Combining the results from FTIR and EDS analysis, the composition of the film is best described as $\text{Zn}_{0.61}\text{Al}_{0.39}(\text{OH})_2(\text{NO}_3)_{0.39} \cdot x\text{H}_2\text{O}$. The Zn^{2+} to Al^{3+} ratio in this film appears to be the only Zn^{2+} to Al^{3+} ratio that can be obtained by our condition. Any attempt to decrease the Al^{3+} content in the film by increasing the Zn^{2+} to Al^{3+} ratios in the plating solution resulted in the formation of zinc-containing impurities (zinc oxide and zinc hydroxide).

(25) Klopogge, J. T.; Wharton, D.; Hickey, L.; Frost, R. L. *Am. Mineral.* **2002**, *87*, 623.

(26) Sun, W.; He, Q.; Luo, Y. *Mater. Lett.* **2007**, *61*, 1881.

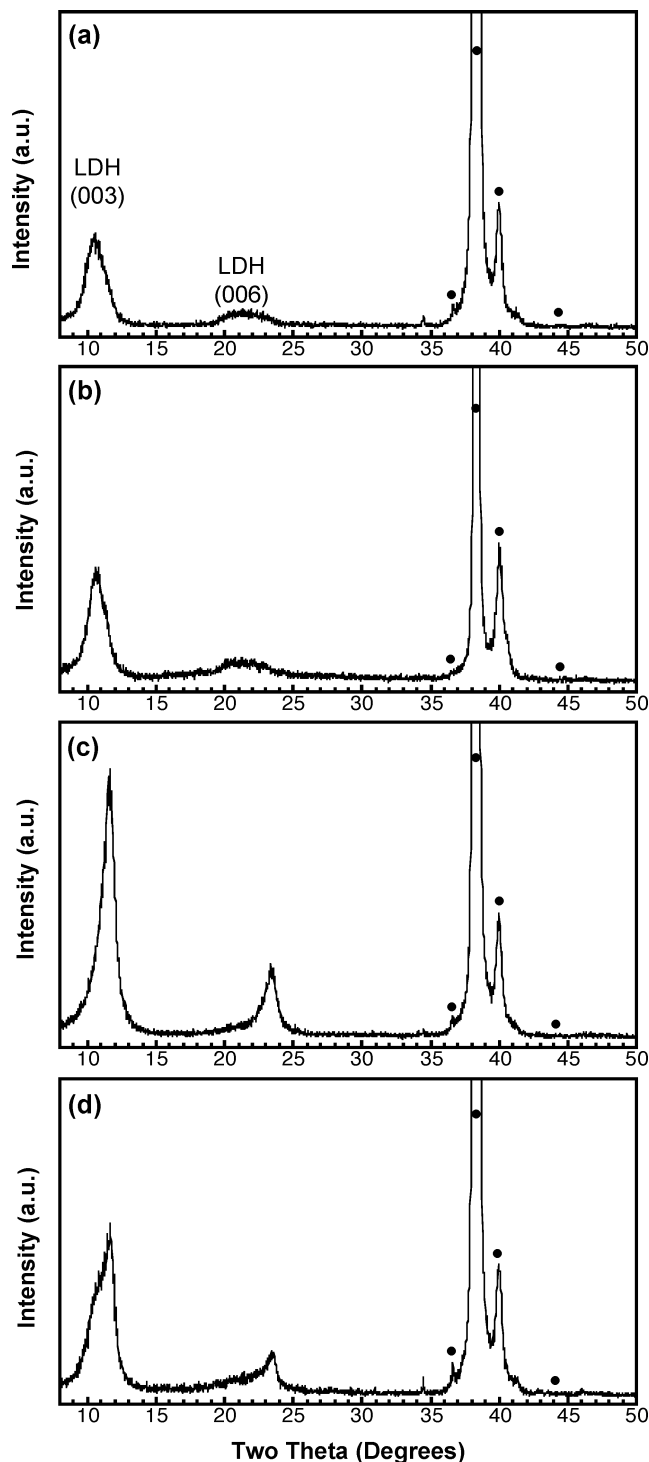


Figure 4. XRD of the films deposited from Solution II at (a) -1.5 V, (b) $E = -1.6$ V, (c) $E = -1.65$ V, and (d) $E = -1.7$ V. The XRD patterns shown in part b of Figure 4 and in part b of Figure 3 are identical, but this pattern is shown again here for easy comparison of the effect of deposition potential. Peaks generated by the gold substrate are marked as (*).

Conclusions

We have identified an electrochemical condition to produce Zn–Al LDH films. Obtaining pure Zn–Al LDH films required successfully suppressing deposition of zinc oxide and zinc hydroxide in addition to zinc metal and aluminum impurities. Deposition was carried out at room temperature, which favors deposition of zinc hydroxide over deposition

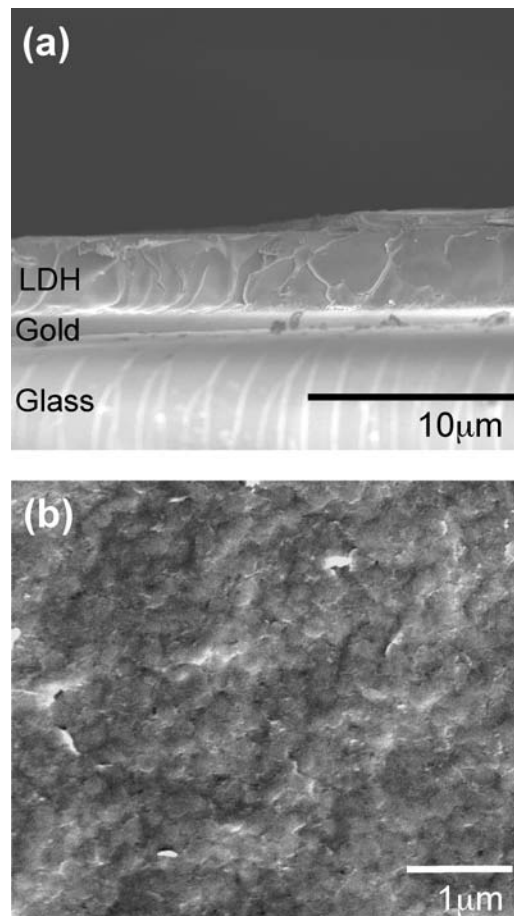


Figure 5. SEM images showing (a) the side view and (b) top view of Zn–Al LDH films deposited from solution II (pH 3.8) at $E = -1.65$ V.

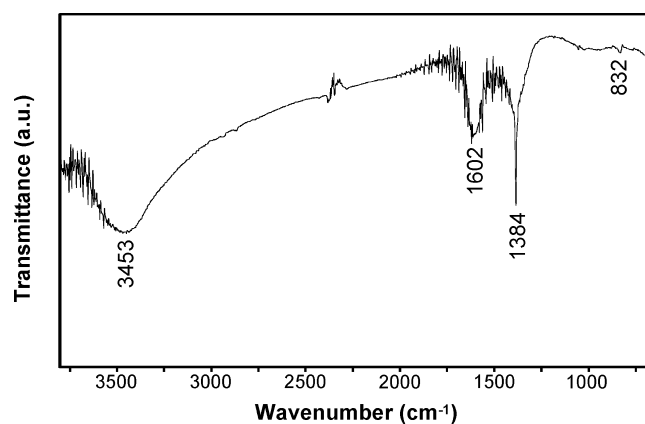


Figure 6. FTIR spectrum of the LDH film deposited from solution II (pH 3.8) at $E = -1.65$ V.

of zinc oxide in general. The deposition potential was chosen to allow for the reduction of nitrate ions but not for the reduction of Zn^{2+} or Al^{3+} ions. Hydroxide phases were obtained as the major phase between $E = -1.5$ V and $E = -1.65$ V. Making the deposition potential more positive or negative resulted in deposition of zinc oxide or zinc metal, respectively. Forming a pure Zn–Al LDH phase required an appropriate Zn^{2+} to Al^{3+} ratio in the plating solution. Deviation from the optimum solution composition resulted in formation of Zn- or Al-containing impurities in the films. The most crystalline and pure Zn–Al LDH film was obtained

at $E = -1.65$ V, using a solution containing 12.5 mM $\text{Zn}(\text{NO}_3)_2 \cdot 6\text{H}_2\text{O}$ and 7.5 mM $\text{Al}(\text{NO}_3)_3 \cdot 9\text{H}_2\text{O}$ (pH was adjusted to 3.8). The resulting film contained 39 atomic % Al^{3+} ions replacing Zn^{2+} ions, leading to a composition of $\text{Zn}_{0.61}\text{Al}_{0.39}(\text{OH})_2(\text{NO}_3)_{0.39} \cdot x\text{H}_2\text{O}$.

The synthesis method described here provides a facile and efficient way to produce Zn–Al LDH films. The optimum condition identified in this study can further be modified to

-
- (27) Chen, H. Y.; Zhang, F. Z.; Fu, S. S.; Duan, X. *Adv. Mater.* **2006**, *18*, 3089.
(28) Gardner, E.; Huntoon, K. M.; Pinnavaia, T. J. *Adv. Mater.* **2001**, *13*, 1263.
(29) Lee, J. H.; Rhee, S. W.; Jung, D. Y. *Chem. Commun.* **2003**, 2740.
(30) Lee, J. H.; Rhee, S. W.; Jung, D. Y. *Chem. Mater.* **2004**, *16*, 3774.
(31) Lee, J. H.; Rhee, S. W.; Jung, D. Y. *J. Am. Chem. Soc.* **2007**, *129*, 3522.

obtain desired nano- and microscale morphologies of LDH films (domain size, packing orientation, porosity, surface texture), which is an important issue to address to enhance desired reactivities or stabilities of LDH films.^{27–31} In addition, this electrodeposition method can create new opportunities to prepare composite Zn–Al electrodes containing various interlayer species by a facile one-step procedure.

Acknowledgment. This work was supported by the U.S. Department of Energy (DE-FG02-05ER15752) and the Alfred P. Sloan Foundation. It made use of the Life Science Microscopy Facility at Purdue University.

IC800193J